International Journal of Coal Science & Technology (2023) 10:68
https://doi.org/10.1007/s40789-023-00616-2

RESEARCH

Time-shift effect of spontaneous combustion characteristics and microstructure difference of dry-soaked coal

Yikang Liu[2] · Haiyan Wang[1] · Huiyong Niu[2] · Tao Wang[2] · Zhiwen Chen[2] · Yuqi Chen[2] · Qingjie Qi[3]

Received: 18 June 2023 / Revised: 24 July 2023 / Accepted: 2 August 2023

Abstract

The physical and chemical properties of the air-dried residual coal after soaking in the goaf will change, resulting in an increase in its spontaneous combustion tendency. This study aimed to look into the features and mechanism of soaked-dried coal's spontaneous combustion. Five samples of coal were dried to various degrees, and the weight loss features during thermal processing were examined. Based on this, the pore structure and chemical structure characteristics of the coal samples with the highest tendency to spontaneous combustion were quantitatively examined, and the mechanism by which soaking-drying affected the spontaneous combustion heating process of the remaining coal in goaf was investigated in turn. The results show that T_1 decreases with the increase of drying time, T_2–T_6 shows a fluctuating change, and the ignition activation energy of 36-S-Coal is smaller than that of other coal samples. The pore type of 36-S-Coal changes from a one-end closed impermeable pore to an open pore, and the pore group area is large. During the 36 h drying process, the internal channels of the coal were dredged, and a large number of gravels and minerals were precipitated from the pores with the air flow. A large number of gravels were around the pores to form a surface structure that was easy to adsorb various gases. Furthermore, infrared spectroscopy was used to analyze the two coal samples. It was found that soaking and drying did not change the functional group types of coal samples, but the fatty chain degree of 36-S-Coal was reduced to 1.56. It shows that the aliphatic chain structure of coal is changed after 36 h of drying after 30 days of soaking, which leads to the continuous shedding of aliphatic chain branches of residual coal, and the skeleton of coal is looser, which makes the low-temperature oxidation reaction of 36-S-Coal easier. Based on the above results, the coal-oxygen composite mechanism of water-immersed-dried coal is obtained, and it is considered that the key to the spontaneous combustion oxidation process of coal is to provide oxygen atoms and accelerate the formation of peroxides.

Keywords Water-soaked coal · Coal spontaneous combustion · FTIR · TG-DTG · Pore structure · Chemical structure parameters

1 Introduction

Coal spontaneous combustion is a severe hazard in mining (Fei et al. 2009; Liang et al. 2023; Niu et al. 2022; Tan et al. 2022; Wang et al. 2021). During coal seam mining, various geological conditions create a large number of airflow cracks, water-conducting, and water-passing cracks on the roof fracture of the goaf (Niu et al. 2022; Wang et al. 2022; Yu et al. 2013). Channel water gushing causes the residual coal in the goaf to form new pores and cracks after soaking, significantly changing the physical structure of residual coal (Pan et al. 2016; Yang et al. 2017). Moreover, soluble substances in coal change their chemical composition under the influence of water, altering the oxidation rate and the coal spontaneous combustion heating process (Huang et al. 2019;

✉ Haiyan Wang
whycumtb@163.com

✉ Huiyong Niu
niuhuiyong@163.com

[1] Research Institute of Macro-Safety Science, University of Science and Technology Beijing, Beijing, China

[2] School of Civil and Resource Engineering, University of Science and Technology Beijing, Beijing, China

[3] Chinese Institute of Coal Science, Beijing, China

Published online: 27 October 2023

Onifade and Genc 2018; Xiaowei et al. 2019; Zeng and Shen 2022; Zhang et al. 2016). As the temperature increases in the goaf, the residual coal dries after soaking. In the presence of elevated oxygen concentration, spontaneous combustion is prone to occur, leading to more severe coal mine fires (Fan et al. 2020; Niu et al. 2022; Shi et al. 2018; Xu et al. 2021; Yang et al. 2017; Zhang et al. 2018). Domestic and international scholars have conducted broad studies on water-logged coal's pore structure and spontaneous combustion properties. Hokyung Choi's experimental results (Choi et al. 2011) showed that the micropore volume of coal after water immersion and drying doubled that of raw coal. After water immersion, Reich (1992) compared and analyzed the surface structure of raw coal with coal samples after water immersion and drying, finding that shallow water forms a film that prevents air and pores from contacting, thereby isolating oxygen. However, as the temperature rises, water evaporates, and part flows through the coal body, resulting in increased fragmentation and porosity. A vast amount of oxygen entering the pores can accelerate the coal combustion reaction. In coal samples after being soaked, Huang's experimental study (Huang et al. 2022) showed that the fraction of micropores reduced, and the number of macropores grew. Sensogut et al. (2007) studied the water-logged coal's spontaneous combustion procedure and found that wet coal is more prone to burning than dry coal. Additionally, Deng et al. (2016); Zhang et al. (2019); Zhao et al. (2019) employed temperature-programmed tests to examine the combustion process properties and gas production of coal samples after immersion and drying. The results indicated that water immersion drying increased the characteristic temperature. Odeh (2015) concluded that the functional groups of coal tend to evolve in stages with increasing coal metamorphism, leading to the shedding of functional groups. sGhosh and Bandopadhyay (2020) discovered that aliphatic CH- initially increased, then decreased with increasing carbon percentage by FTIR. Furthermore, Liu (2022) observed that with increased temperature, C–C and H–H bonds in coal increased, while C–O bonds decreased. The above research results show that the change of pore structure caused by water immersion affects the spontaneous combustion characteristics of coal. However, the spontaneous combustion process of coal with different drying time was analyzed by thermogravimetric method, and the microscopic pore structure, functional group and chemical structure parameters of coal with the highest natural tendency were further analyzed, so as to infer the coal-oxygen composite mechanism of water-immersed drying coal needs further study.

In view of this, the bituminous coal obtained from Gaojiapu Coal Mine in Shaanxi Province was used as the test coal sample. The spontaneous combustion heating process and activation energy of coal with different drying time after 30 days of soaking were analyzed, and the pore structure development characteristics and chemical structure parameters of coal with the highest natural tendency were further studied. The coal-oxygen composite mechanism of water-immersed-dried residual coal is summarized, which aims to provide theoretical support for controlling the spontaneous combustion of water-immersed-dried residual coal in goaf.

2 Experiment

2.1 Sample collection and preparation

The presence of surface water and rock strata endows the coal seam and goaf with water immersion characteristics, making Gaojiapu coal samples particularly valuable for studying spontaneous combustion characteristics in water-immersed and dry coal.Once collected on-site, the coal samples were meticulously packaged and sent to the laboratory, conforming to standard protocols. After the outer layers of the coal seam were stripped, a crusher was used for crushing and screening, with coal particles sized at 0.27–0.55 nm selected and duly sealed for preservation. The coal seam was soaked in distilled water for 30 days and labeled with the number and date. The equipment necessary for coal sample collection, preparation, and experimentation is illustrated in Fig. 1

2.2 Experimental test

After soaking for 30 days, the coal samples were removed, laid flat on drying trays, and left to stand for 30 min, during which time excess moisture was extracted using paper towels. When the coal sample has no apparent water outflow, it is divided into five parts, of which four parts are then placed in a drum-drying oven to dry. Every 12 h, samples were obtained while the drying process was underway at 30 °C. Samples were taken at 12-h intervals and stored in a sealed container after removal. The coal samples used in this experiment were numbered as follows: R-Coal (Raw coal sample), 12-S-Coal (Dried for 12 h after water immersion), 24-S-Coal (Dried for 24 h after water immersion), 36-S-Coal (Dried for 36 h after water immersion) and 48-S-Coal (Dried for 48 h after water immersion). The coal sample preparation process and experimental test flow are shown in Fig. 2.

The thermal analyzer analyzed the thermal weight loss of coal samples. The initial temperature was set to room temperature, the heating rate was 10 °C/min, the end temperature was 1000 °C, the mass of the coal sample was 15 (± 1) mg, and the volume fraction of oxygen was 21%.

A high-power electron scanning microscope observed the surface morphology distribution and change of coal samples under different drying times. Five groups of coal samples sealed in sealed bags were prepared according to the sample

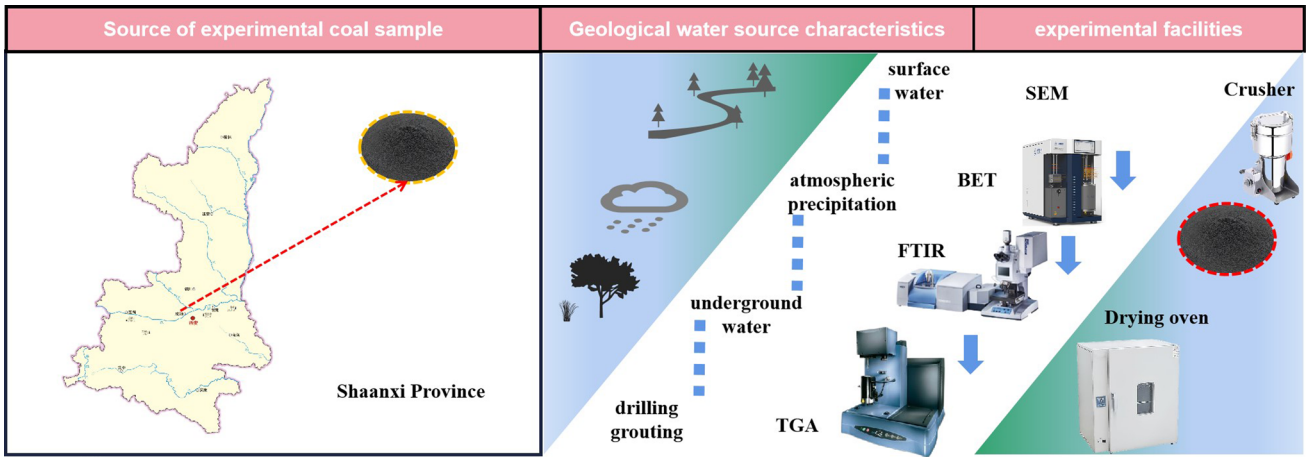

Fig. 1 Diagram of coal sample collection and preparation

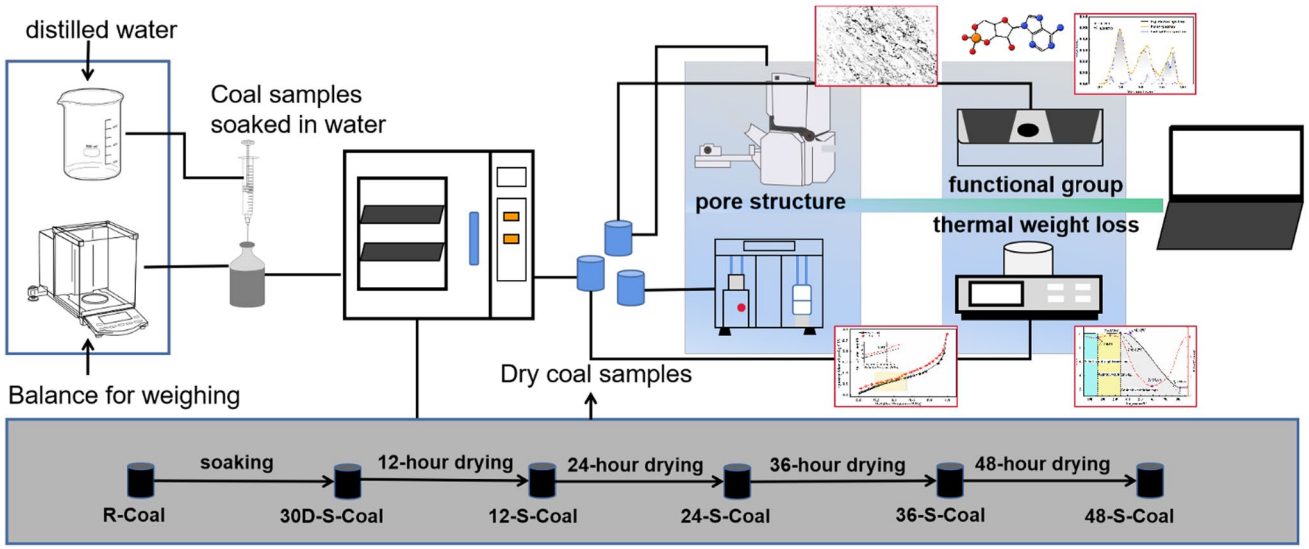

Fig. 2 Experimental test flow chart

standard of the scanning electron microscope experiment. In order to improve electrical conductivity, firstly, all coal samples are glued to the conductive belt in a specific order. Then the coal samples on the conductive belt are sprayed with gold so that the coal samples, after spraying gold, are stabilized. Please put it on the observation platform in the test sample room, set the magnification to 1000 times, and scan it.

The microstructure and pore types of coal samples were evaluated through the usage of the liquid nitrogen adsorption method at low temperatures. Firstly, the sample tube was weighed, and the residual water in the coal pores was removed by high-temperature degassing. Then, the relevant parameters were set, and the protective cover was installed for testing.

The change in the functional group composition of coal samples was examined using an infrared spectrometer. The sample was created using the tableting technique for potassium bromide. Dry KBr was added to the coal sample in a ratio of 1:180, and the mixture was subsequently pulverized. Once thoroughly mixed, the coal-KBr mixture was compressed into a transparent sheet using a die press. This sheet was then scanned using infrared spectrometry to obtain a Fourier infrared spectrum for each coal sample.

3 Results and discussion

3.1 Analysis of thermal weight loss characteristics of coal with different drying time

Soaking can alter dry coal's physical properties and chemical structure, leading to a complicated impact on the spontaneous combustion and oxidation process (Wang 2012). The oxidation features of spontaneous coal combustion were analyzed using a thermogravimetric analyzer to examine the impact of various drying times. After the experiment, the TG-DTG curve was output. The change rate of coal sample quality can be obtained by differentiating the temperature and then multiplying the growth rate. The curve represents the rate of change of the total mass of the coal sample during heating.

T_1 (dehydration temperature point), T_2 (growth temperature point), T_3 (oxygen absorption temperature point), T_4 (ignition temperature point), T_5 (maximum weight loss rate temperature point), and T_6 (burnout temperature point) were the six distinct temperature points on the heating curve that were selected to investigate the heating and oxidation traits of various dry coal samples (Qi et al. 2017). Similarly, the whole heating process is divided into the dehydration weight loss stage (initial temperature ~ T_1), oxidation weight gain stage (T_1–T_3), and combustion weight loss stage (T_3–T_6) (Deng et al. 2018). The TG-DTG curve of the coal sample is shown in Fig. 1.

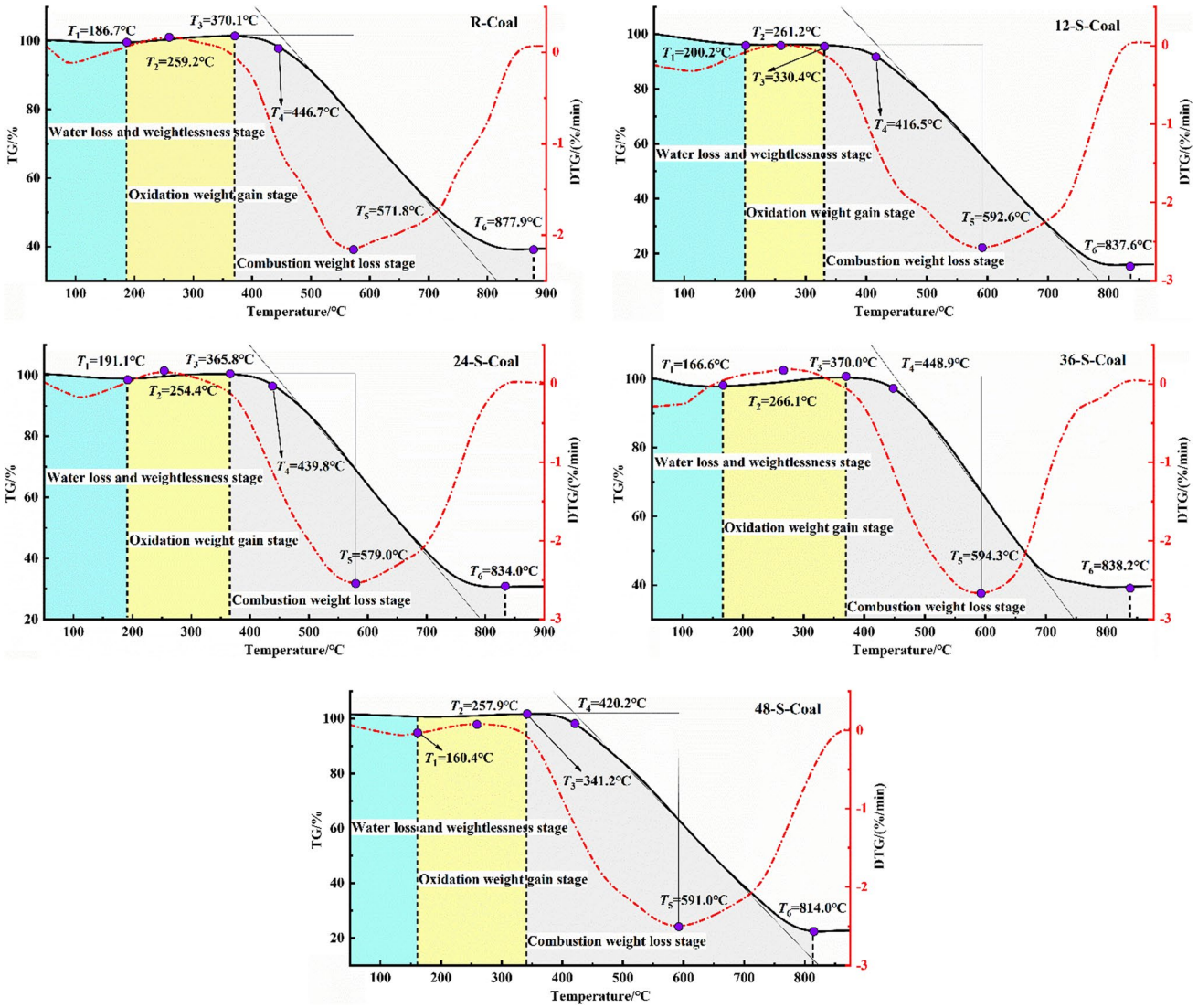

Fig. 3 TG-DTG curve

Figure 3 shows that each coal sample's characteristic temperature points and stages show different patterns. In order to obtain more clearly the influence of the drying time on the spontaneous burning process of the coal, the change in the characteristic temperature points is analyzed, as shown in Fig. 4.

It can be seen from Fig. 4 that T_1 decreases with the increase in drying time, indicating that drying time affects pore water loss and gas flow. T_2–T_6 showed fluctuating changes, but the temperature of 36-S-Coal was higher than that of other coal samples. This indicates that the coal sample reaches the best spontaneous combustion dryness after drying for 36 h. However, only the size of the characteristic temperature point demonstrates that the spontaneous combustion tendency is not rigorous. Therefore, combined with the characteristic temperature section and the thermal weight loss process, the activation energy of the characteristic stage of different coal samples is calculated (Song et al. 2019).

The solution process is as follows: firstly, the mass change rate α of the coal sample is obtained, which is expressed as Eq. (1), and then the differential form Eq. (2) and integral form Eq. (3) of the reaction rate are obtained by analyzing the reaction process, and the relationship between $g(\alpha)$ and $f(\alpha)$ is obtained as (4). Since the temperature changes with time when Eqs. (2) and (3) are applied, Eq. (5) needs to be satisfied. The integral form Eq. (6) of the non-isothermal equation can be obtained by Eqs. (2) and (5). The Coast-Redfern integral method solves Eqs. (7) and (8) (Yang et al. 2019).

$$\alpha = \frac{m_0 - m}{m_0} = \frac{\Delta m}{m_0} \tag{1}$$

$$\frac{\mathrm{d}\alpha}{\mathrm{d}t} = kf(\alpha) \tag{2}$$

$$g(\alpha) = kt \tag{3}$$

$$f(\alpha) = \frac{1}{g'(\alpha)} = \frac{1}{\mathrm{d}\left[g(\alpha)\right]/\mathrm{d}\alpha} \tag{4}$$

$$k = A \cdot e^{-\frac{E}{RT}} \tag{5}$$

$$T = T_0 + \beta t \tag{6}$$

$$g(a) = \int_0^{\alpha} \frac{\mathrm{d}\alpha}{f(\alpha)} = \frac{A}{\beta}\int_{T_0}^{T} e^{-\frac{E}{RT}}\mathrm{d}T = \frac{A}{\beta}\int_0^{T} e^{-\frac{E}{RT}}\mathrm{d}T \tag{7}$$

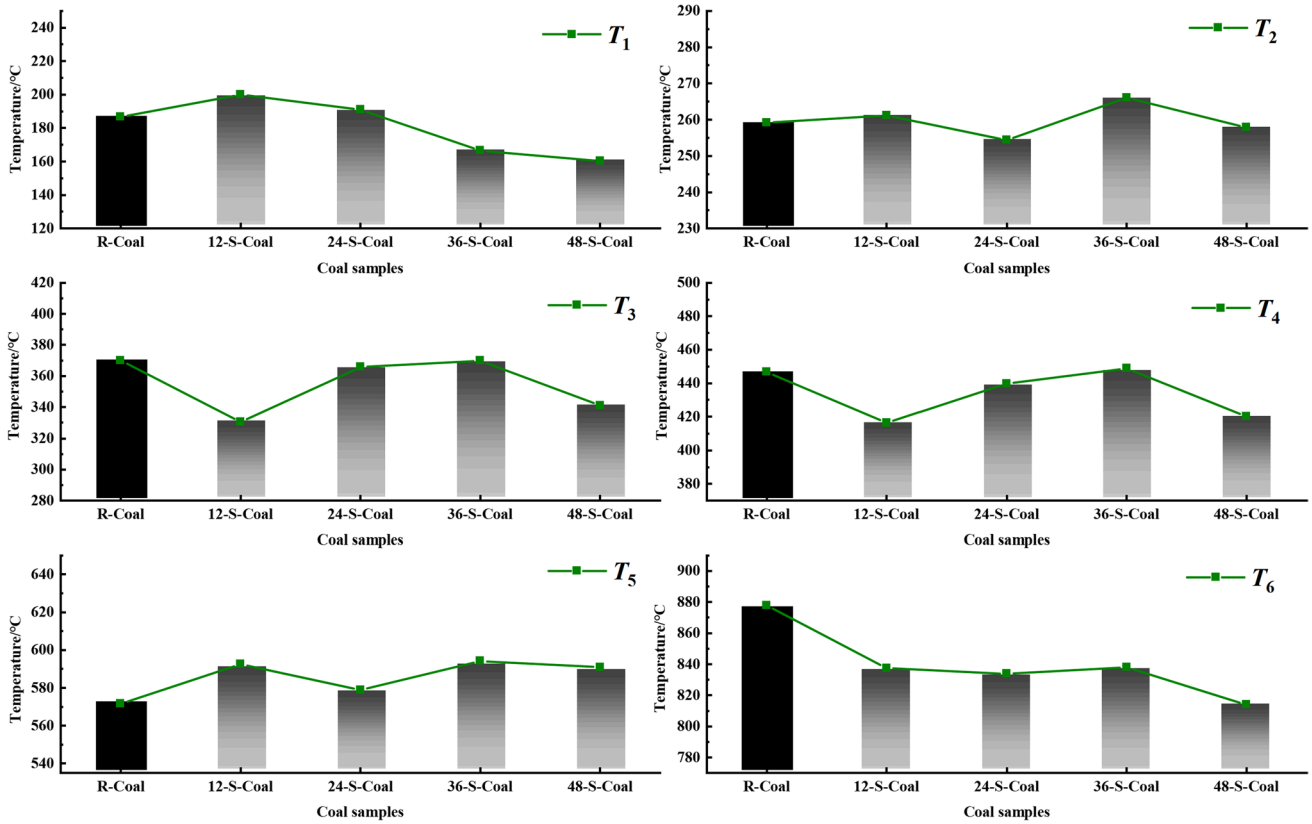

Fig. 4 R-Coal and characteristic temperature point change curves for coal at different drying times

$$\ln\left[\frac{g(\alpha)}{T^2}\right] = \ln\left[\frac{AR}{\beta E}\right] - \frac{E}{RT} \tag{8}$$

where, m_0 is the initial mass, g; m is the quality of a certain moment, g; m_∞ is the final residual mass of the coal sample, g; Δm is the mass loss of the coal sample at any time, g; k is the reaction rate constant; A is the pre-exponential factor; E is the activation energy, kJ/mol; T is Kjeldahl temperature, K; R is the molar gas constant, 8.314 J/ min K; β is the heating rate, K/ min; T_0 is the temperature at which weight loss begins, K.

When $n=1$, $\ln\left[\frac{1-(1-\alpha)^{1-n}}{T^2(1-n)}\right]$ is plotted against $\frac{1}{T}$, when $n=1$, $\ln\left[\frac{-\ln(1-\alpha)}{T^2}\right]$ is plotted against $\frac{1}{T}$, the slope k obtained is $-\frac{E}{R}$, and the intercept is $\ln\frac{AR}{\beta E}$. By bringing the different mechanism function into the equation for analysis, it is possible to find E.

The activation energy calculation results of different stages are shown in Table 1. The tendency for spontaneous combustion is more substantial, the lower the activating energy. According to the data in Table 1, 48-S-Coal has higher activation energy than 24-S-Coal, R-Coal, 12-S-Coal, and 36-S-Coal during the dehydration phase. The activation energy of the oxygen absorption weight gain stage is 12-S-Coal > 24-S-Coal > R-Coal > 48-S-Coal > 36-S-Coal. The activation energy of the combustion weight loss stage is 24-S-Coal > R-Coal > 48-S-Coal > 36-S-Coal > 12-S-Coa l. The activation energy obtained in the oxygen absorption weight gain stage represents the ignition activation energy in the combustion process of the coal sample, and the activation energy obtained in the combustion weight loss stage represents the combustion activation energy in the combustion process of the coal sample. In this study, the ignition activation energy can more accurately reflect the difficulty of spontaneous combustion of coal samples. Therefore, it can be concluded that the natural tendency of coal samples in this study does not increase with the increase of drying time, and 36-S coal has a higher tendency of spontaneous combustion.

3.2 Analysis of coal pore group distribution

Based on the thermogravimetric analysis, it is concluded that 36-S-Coal has a higher spontaneous combustion tendency. Coal is a complex solid material with porous media. It has expansion characteristics and a developed internal pore structure, increasing the probability of contact between organic matter in coal and external gas and providing a large contact area for the coal-oxygen mixed reaction (Li et al. 2023; Yu et al. 2013). Therefore, to observe the influence of soaking and drying on the morphology of coal more intuitively, the pore fracture distribution of R-Coal and 36-S-Coal was analyzed by scanning electron microscopy, as shown in Fig. 5. The area surrounded by red (a–c) and blue (d–f) in Fig. 5 represents the distribution of pore groups and fracture groups of raw coal and 36-S-Coal coal samples, and contain a large number of gravel filling in these areas.

Coal contains more minerals and has a complex structure. The minerals distributed on the surface of coal account for only a part of these minerals, and another amount of the minerals are present inside the coal (Li et al. 2019). According to the scanning results, the SEM image is gray-scale adjusted, and the pore group in the image is highlighted to obtain the pore development degree of the coal sample after soaking. It can be seen from Fig. 5a–c that the surface of R-Coal is relatively smooth, the number of pores and cracks

Table 1 Activation energy of coal samples at different stages

Coal sample	Reaction stage	Temperature range (°)	Activation energy (kJ/mol)
R-Coal	Water-loss and weight-loss stage	50.0–186.7	42.9
	Oxygenated weight gain stage	186.7–370.1	117.8
	Burning weightless stage	370.1–877.9	54.0
12-S-Coal	Water-loss and weight-loss stage	50.0–200.2	40.8
	Oxygenated weight gain stage	200.2–330.4	163.1
	Burning weightless stage	330.4–837.6	24.6
24-S-Coal	Water-loss and weight-loss stage	50.0–191.1	43.0
	Oxygenated weight gain stage	191.1–365.8	123.3
	Burning weightless stage	365.8–834.0	56.1
36-S-Coal	Water-loss and weight-loss stage	50.0–166.6	40.7
	Oxygenated weight gain stage	166.6–370.0	101.8
	Burning weightless stage	370.0–838.2	48.0
48-S-Coal	Water-loss and weight-loss stage	50.0–160.4	44.5
	Oxygenated weight gain stage	160.4–341.2	112.1
	Burning weightless stage	341.2–814.0	50.2

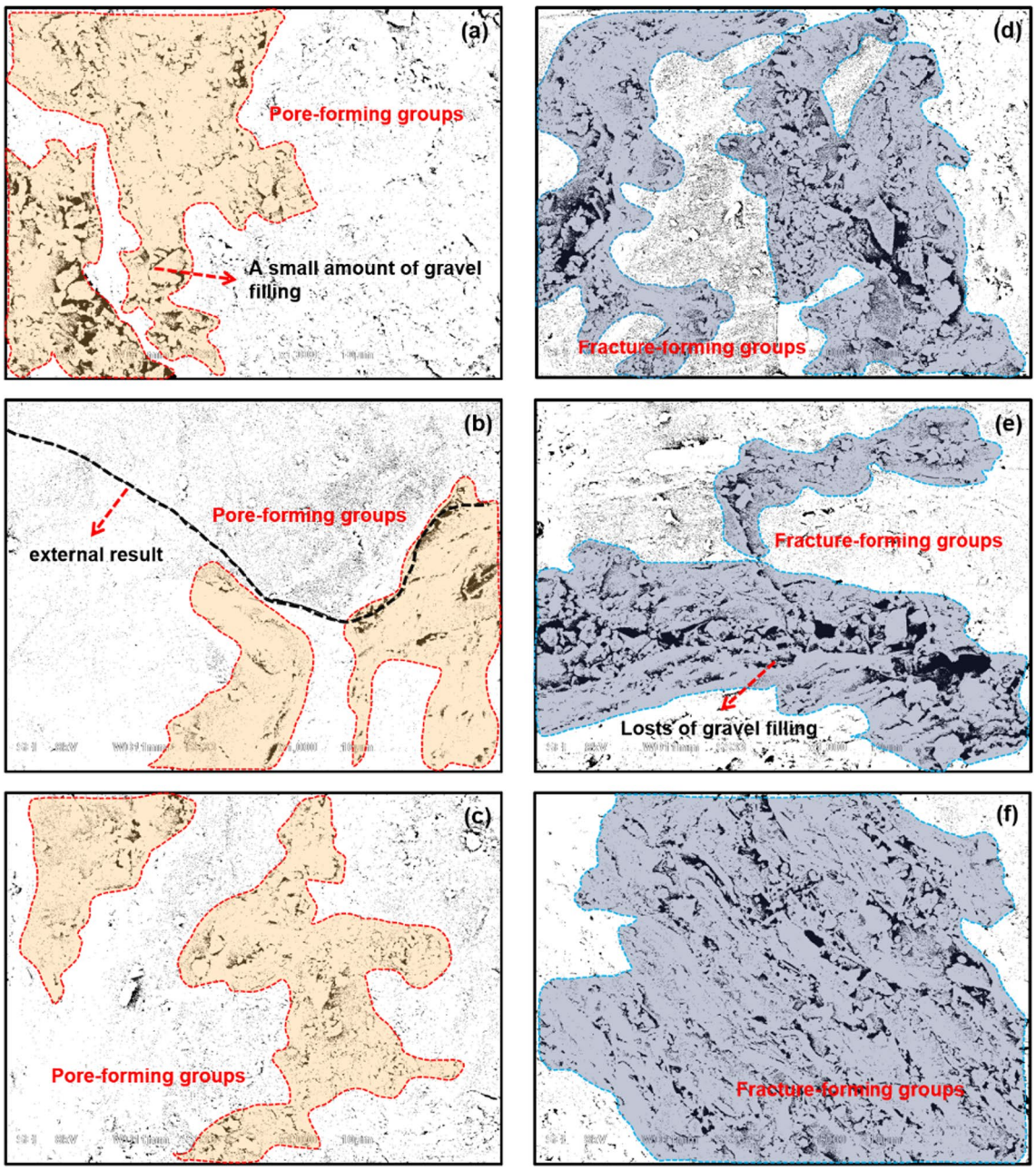

Fig. 5 SEM images of R-Coal and 36-S-Coal samples. **a–c** is the pore structure diagram of R-Coal, **d–f** is the pore structure diagram of 36-S-Coal

is small, the proportion of pore group area is low, and a small amount of gravel is attached to the coal surface and around the cracks. The crack in Fig. 5b is likely caused by the external force during crushing. After 30 days of soaking, the pore cracks of coal samples are well developed. It can be seen from Fig. 5d–f that the water immersion strengthens the fracture of the original coal structure, dredges the pores containing loose minerals, and further evolves into swelling pores, increasing the internal pores.

Further analysis found that during the 36 h drying process, the internal channels of coal pores were dredged. At this time, a large amount of gravel and minerals are precipitated from the pores as the air flow, resulting in a large amount of gravel around the pore group. It is obvious to see that the number of pores in the coal dried for 36 h after soaking for 30 days is relatively increased, and the porosity of the coal body increases, and the proportion of the pore group area also increases. At this time, the coal body forms a surface structure that is easy to adsorb various gases, which

leads to an increase in the possibility of oxygen adsorption by the coal body, and further enhances the oxygen adsorption capacity in the process of coal oxidation. This further indicates that 36-S-coal has a higher possibility of spontaneous combustion than R-coal, which is consistent with the conclusion of thermogravimetric experiment.

3.3 Analysis of variations in coal pore types

On the basis of the pore structure distribution analysis, the pore types of the coal samples were analyzed using a low-temperature liquid nitrogen adsorption experiment. Simultaneously, the conclusion of the thermogravimetric investigation was verified. The adsorption experiment of liquid nitrogen at low temperatures is the adsorption process of pressurized nitrogen. In this process, the adsorption follows the order of micropores, micropores, mesopores, and macropores, and the adsorption principle of transition from single-layer to multi-layer delayed adsorption. The curve shape formed in this process reflects the morphological structure of the coal sample hole. Based on this experiment, IUPAC divides the pores into micropores (pore size 50 nm) according to the pore diameter and divides the adsorption isotherm curve into 6 categories (Thommes et al. 2015), as shown in Fig. 6.

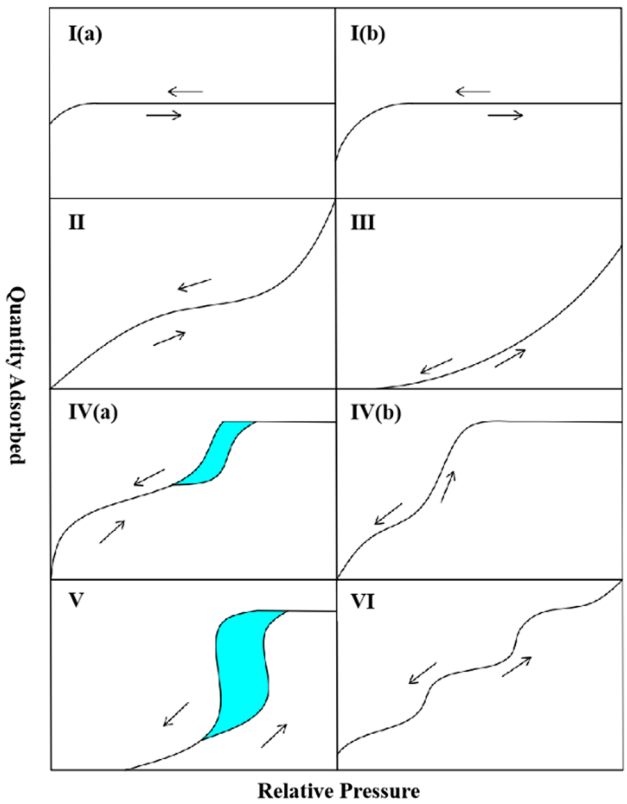

Fig. 6 Classification of adsorption isotherm curves (IUPAC)

According to the classification characteristics of isothermal adsorption curves, the type of adsorption isotherm curve (a) of R-Coal is between III and IV (a), which can be classified as IV (a), and the adsorption isotherm curve (b) of 36-S-Coal belongs to V type.

It can be seen from Fig. 4a that the loop of the R-Coal curve is tiny, and there is no obvious inflection point when the relative pressure is slight, and there is a weak hysteresis loop. This is due to the continuous filling of coal micropores during nitrogen adsorption. It is reasonable to presume that the R-Coal sample's pore type is predominantly made up of closed, impermeable pores at one end. The desorption curve on the 36-S-Coal curve displays a distinct inflection point of about 0.5, as seen in Fig. 4b. There is a typical hysteresis loop between the adsorption curve and the desorption curve. According to the above analysis, the pore type of coal sample developed from an impermeable pore to an open pore after 30 days of soaking and 36 h of drying. It can be explained that under underwater immersion, soluble substances in coal are dissolved, and the connecting channel between pores is opened. After 36 h of drying, the air permeability of coal samples is further enhanced. Pore-type switching from impermeable to open pores encourages O_2 circulation in coal, increasing the coal and oxygen contact area. The open pores of coal are broken due to the temperature rise, and the normal pore expansion phenomenon manifests, increasing the likelihood that the coal-oxygen combination effect will occur (Fig. 7).

3.4 Analysis of changes in functional groups of coal

The oxidation process of coal is essentially a process in which different types of groups in coal undergo oxidative decomposition reactions and release heat (Zhao et al. 2022). These groups continuously react to release heat and activate more groups to respond, so the coal temperature continues to increase until it reaches the point where the coal sample ignites (Chen et al. 2012; Dey 2012; Li et al. 2017). When the number of functional groups in coal molecules changes, the intensity of its infrared absorption peak will change accordingly. Thus, analyzing the infrared spectrum curve makes it possible to determine the distribution of different functional groups in the coal sample and analyze the impact of drying time on the effectiveness of the coal oxygen reaction. Figure 8 displays the infrared spectra of coal samples dried at various rates.

It can be seen from Fig. 8 that the two coal samples have characteristic peaks at 1050 cm^{-1}, 1430 cm^{-1}, 1610 cm^{-1}, 2920 cm^{-1}, and 3460–3730 cm^{-1}, but the wavelength corresponding to the characteristic peaks does not change. In the characteristic absorption region of 1430 cm^{-1}–1660 cm^{-1}, both R-Coal and 36-S-Coal showed strong absorption peaks. This is because the pore structure on the surface of the coal

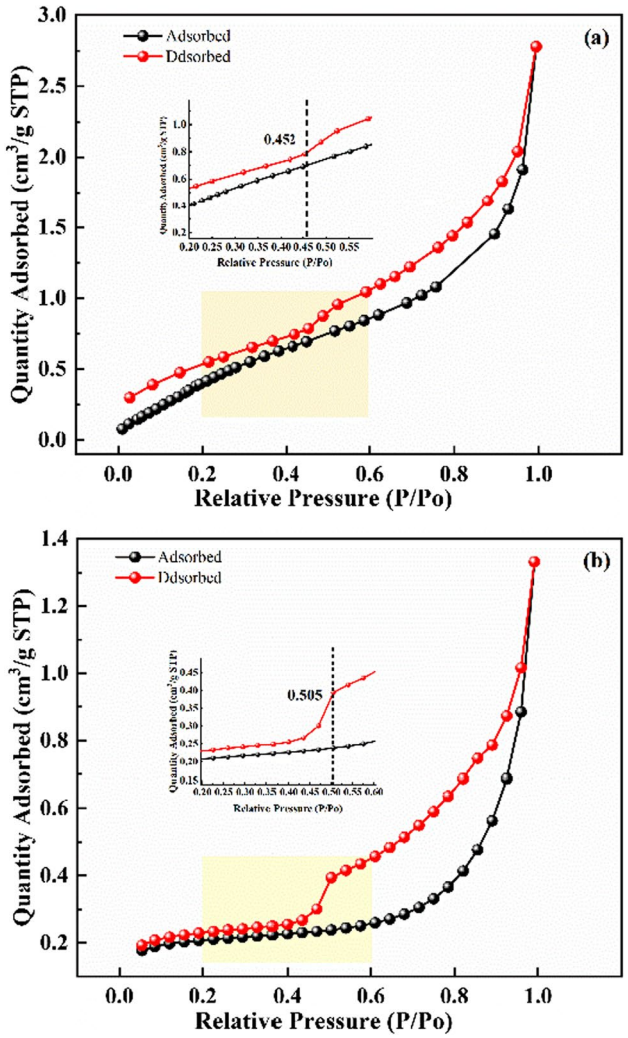

Fig. 7 R-Coal and 36-S-Coal adsorption isotherm curves

sample is affected by the swelling of the water, and the sizeable cross-linked structure and the fat branch chain inside the coal are destroyed, destroying the surface pores. The infrared spectrum shows that immersion and drying do not cause a wide variety of changes in the functional groups of coal samples.

3.4.1 Split-peak fitting

In order to improve the accuracy of the analysis, the infrared spectrum in the range of 700–3700 cm^{-1} was segmented. Then, Peakfit software was used for peak separation and fitting to obtain the characteristic peak data of oxygen-containing functional groups in coal molecules (Zhou et al. 2015). An infrared comparative analysis of R-Coal and 36-S-Coal confirmed that soaking and drying have a negligible impact on the types of functional groups in the raw coal. Further investigation is required to determine whether this process affects the absorption peak area of functional groups. The study has identified several functional groups, including hydroxyl, aliphatic hydrocarbons, aromatic hydrocarbons, and oxygen-containing functional groups, that could potentially affect the coal-oxygen reaction(Zhong et al. 2019). Therefore, the characteristic peaks of different bands (700–900 cm^{-1}, 1000–1800 cm^{-1}, 2800–3000 cm^{-1}, 3000–3700 cm^{-1}) of R-Coal and 36-S-Coal were fitted, as shown in Fig. 9. And the content and proportion of other functional groups are obtained, as shown in Table 2.

The analysis of the relevant results of different band characteristic peaks is shown in Fig. 9. In the 700–900 cm^{-1} band, 14 peaks were fitted, and the correlation was more than 99.8%. 14–15 mounts were included in the 1000–1800 cm^{-1} band, and the correlation was more than 99.8% and 99.7%, respectively. Five peaks were fitted in the

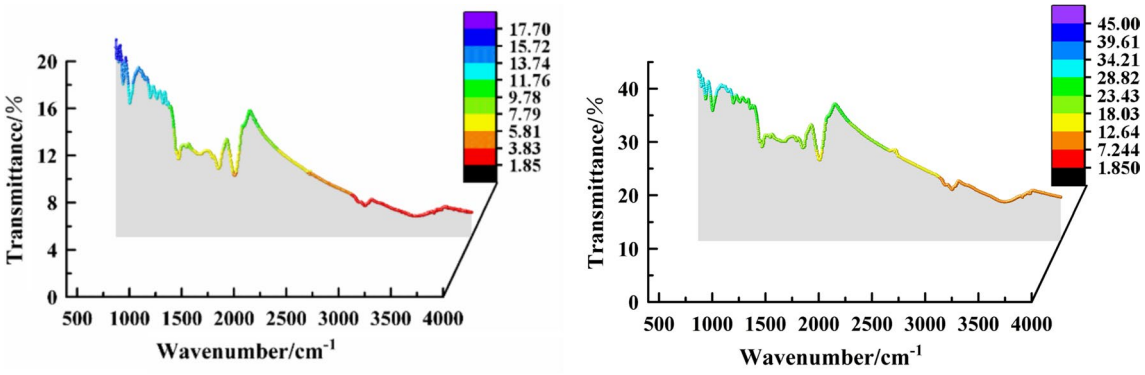

（a）R-Coal （b）36-S-Coal

Fig. 8 Infrared spectra of R-Coal and 36-S-Coal at different drying times

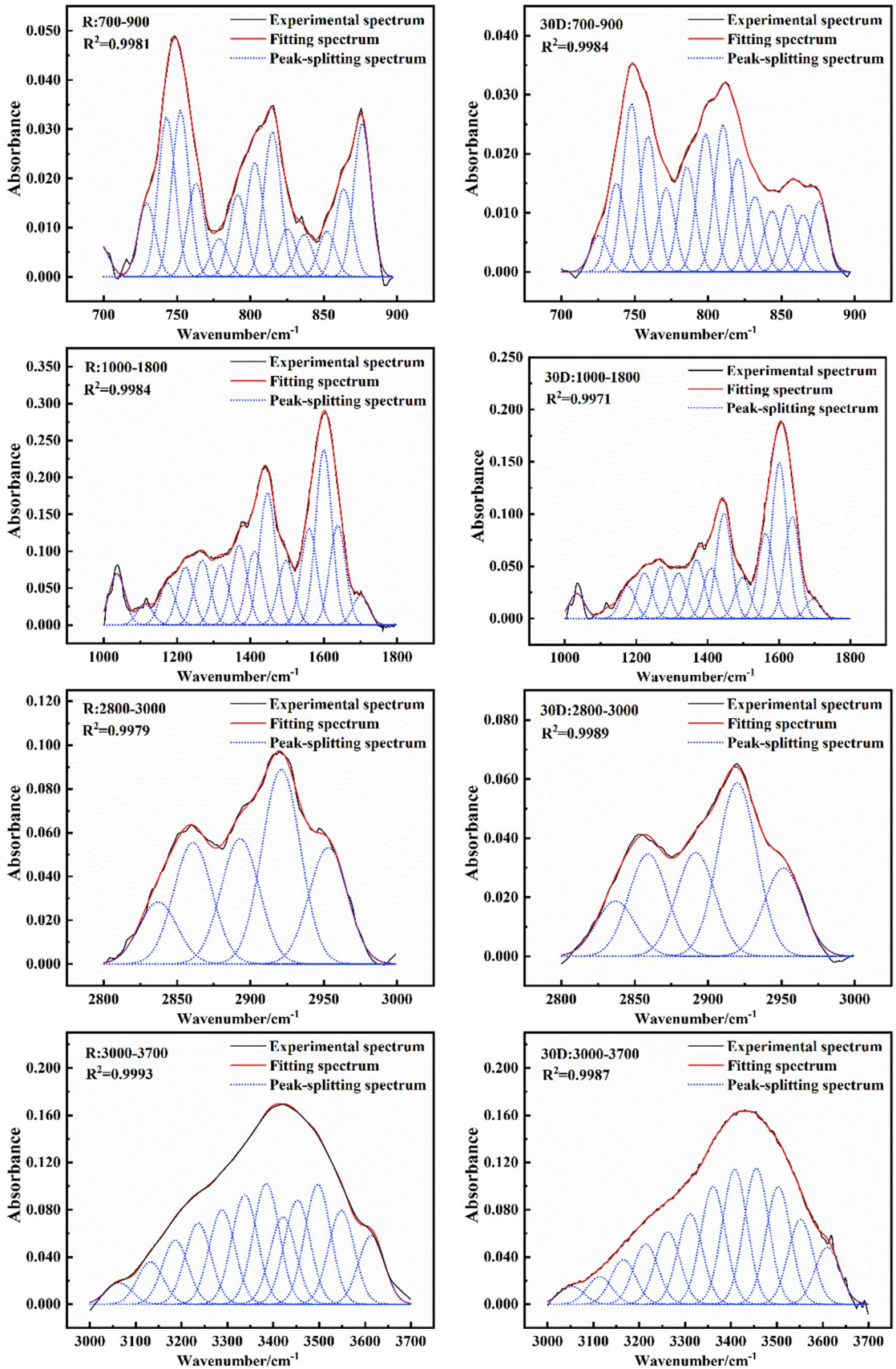

Fig. 9 Infrared spectra of R-Coal and coal samples at different drying times

Table 2 Change in the content of functional groups

Band range	Functional group type	R-Coal (%)	36-S-Coal (%)
700–900cm^{-1}	Phenyl disubstitution	19	22
	Phenylcyclotrisubstitutions	19	45
	Tetraphenyl substitution	39	19
	Phenyl pentacene substitution	23	14
1000–1800cm^{-1}	C-O	28	25
	-CH	33	31
	C = O	36	42
	-COOH	3	2
2800–3000cm^{-1}	-CH_2-(Symmetric stretching vibration)	11	10
	-CH_2-(Antisymmetric stretching vibration)	54	51
	-CH_3(Symmetric stretching vibration)	19	21
	-CH_3(Antisymmetric stretching vibration)	16	18
3000–3700cm^{-1}	Hydrogen bond(-OH and N)	13	9
	Hydrogen bond(O from -OH and C-O)	19	15
	Hydrogen bond(Between molecules)	39	39
	Hydrogen bond(intramolecular)	22	37
	-OH(dissociative)	7	0

2800–3000 cm^{-1} band, with more than 99.7% correlation. In the 3000–3700 cm^{-1} band, 11 mounts were included, and the correlation was more than 99.9% and 99.8%, respectively. In the 700–900 cm^{-1} band, there are four substitution modes on the benzene ring of coal samples, mainly: benzene ring disubstituted (730–750 cm^{-1}), benzene ring trisubstituted (750–810 cm^{-1}), benzene ring tetrasubstituted (810–850 cm^{-1}) and benzene ring pentasubstituted (850–900 cm^{-1}). In the 1000–1800 cm^{-1} band, it is mainly the stretching vibration of oxygen-containing functional groups. In the 2800–3000 cm^{-1} band, there are mainly three types of fats: methyl, methylene, and methine. In the band of 3000–3700 cm^{-1}, hydrogen bonds formed by hydroxyl groups mainly exist in coal.

For calculating the content of a functional group, the sum of the adjusted peak area is considered the total peak area. Then, the percentage of a specific action group about the total area of the peak is determined and used to compute the content of that functional group. Therefore, the area ratio difference of representative functional groups in different bands of R-Coal and water-immersed dry coal samples can be obtained, as shown in Fig. 10.

It can be found from the content and proportion difference of functional groups in different stages that tri-substitution is the primary substitution mode of the benzene ring in the 700–900 cm^{-1} band. Compared with R-Coal, benzene ring disubstitution and benzene ring trisubstituted of 36-S-Coal increased, and the benzene ring pentasubstitution decreased. In the 1000–1800 cm^{-1} band, the content of C–O, methine, and –COOH decreased, and the content of C=O increased. This phenomenon is because the carbon–oxygen single bond is longer than other oxygen-containing functional groups, the chemical properties are unstable, and it is prone to chemical reactions, forming a more stable C=O, making its content increase. In the 2800–3000 cm^{-1} band, the symmetric and antisymmetric stretching vibration of methylene and methyl is the primary vibration mode, manifesting in a decrease in methylene content and an increase in methyl content. In the 3000–3700 cm^{-1} band, the two coal samples' intramolecular hydrogen bonds and intermolecular hydrogen bonds account for about 80% of all hydrogen bonds. However, the difference is that the intramolecular hydrogen bond content of the 36-S-Coal sample increases by 15%, while the intermolecular hydrogen bond content remains unchanged. On the other hand, in the 36-S-Coal coal samples, a decrease was observed in the content of hydrogen bonds formed by the hydroxyl group and N, by the hydroxyl group and O in ether, as well as self-associated hydroxyl groups.

3.4.2 analysis of chemical structure parameters

Water immersion and drying will affect the internal chain reaction of coal. The spontaneous combustion characteristics of coal are impacted by the release of carbon–oxygen and hydrocarbon heat, which is influenced by the chain length and degree of the aliphatic chain during the coal-oxygen chain reaction (Xu et al. 2021). Therefore, this paper analyzes the chain degree and chain length of the fat chain and then studies the difference in spontaneous combustion tendency between the two coal samples.

The fat chain length and branching degree (He et al. 2017; Jiang et al. 2021) were expressed as 'DL-C':

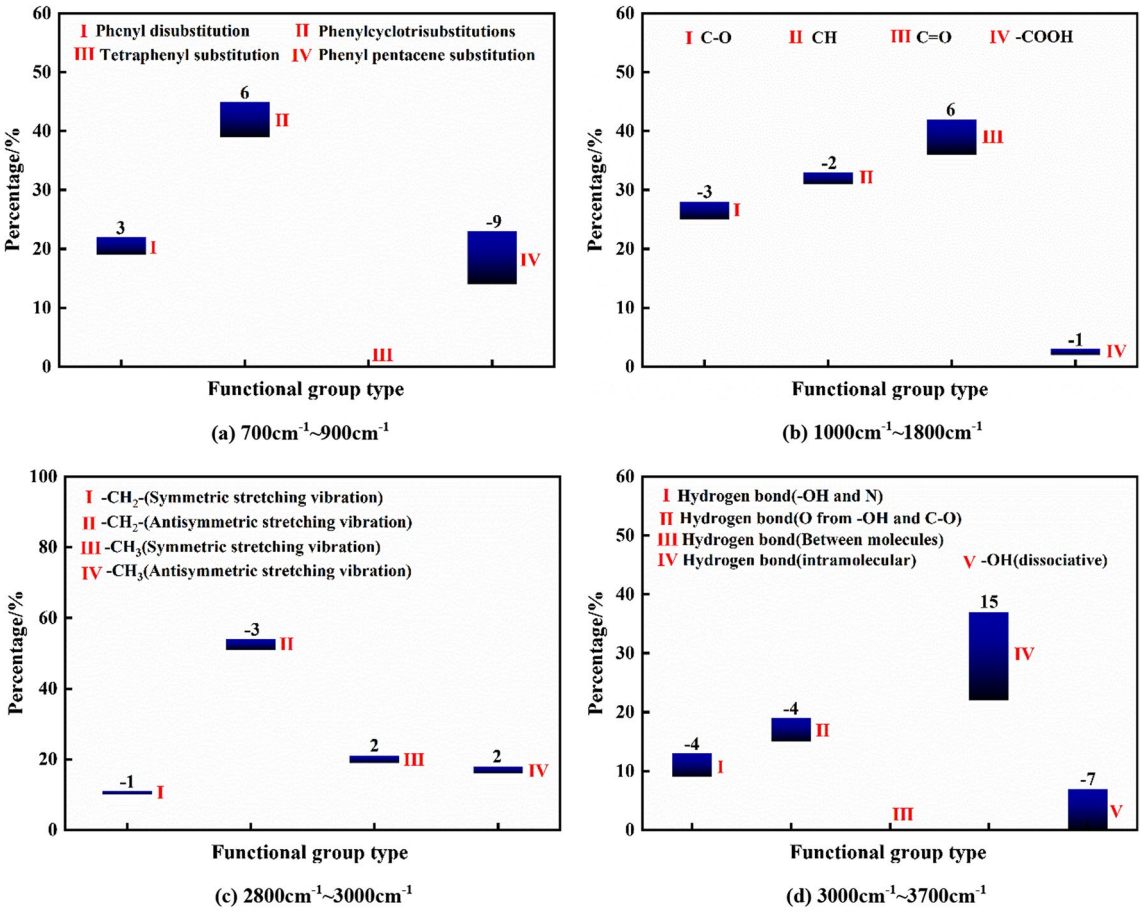

Fig. 10 R-Coal and the difference in the area share of functional groups of coal samples at different drying times

Table 3 Calculated value of coal fat chain length

Coal samples	Fat chain length
R-Coal	1.86
36-S-Coal	1.56

$$'\mathrm{DL}\text{-}\mathrm{C}' = \frac{C1\,(2800-3000)}{C2\,(2800-3000)} \tag{9}$$

where C_1 (2800–3000) is the functional group content of CH_2 in the straight chain portion of aliphatic, the alicyclic and aromatic side chains in the wave count range of 2800–3000 cm^{-1}, %; C_2 (2800–3000) is the functional group content of CH_3 in the branched-chain portion of aliphatic hydrocarbon side chain, alicyclic side chain and the branched part of the aromatic hydrocarbon side chain in the range of 2800–3000 cm^{-1}, %. According to 3.1, the structural parameters of R-Coal and 36-S-Coal were calculated, as shown in Table 3.

It can be seen from Table 3 that 36-S-Coal has a lower level of fat chain formation than R-Coal. This shows that after soaking for 30 d and drying for 36 h, the structure of the aliphatic chain of the coal changes, resulting in the continuous shedding of the residual aliphatic chain branches of the coal and the shortening of the length of the aliphatic chain. At this time, the low-temperature oxidation reaction of 36-S-Coal is easier to achieve.

3.5 Coal-oxygen complex mechanism

Through comprehensive macro and microanalysis, It can be seen that there are apparent differences in functional group content between coal samples immersed in water and raw coal samples. The dryness of coal after submersion into water affects heat and weight loss during the heating process(Fang et al. 2022). Since the oxygen composite reaction is a chemical adsorption-based reaction process, based on the above experimental results, the coal-oxygen composite and chemical adsorption mechanism after water immersion and drying are analyzed, and the coal-oxygen composite model is obtained. As shown in Fig. 11.

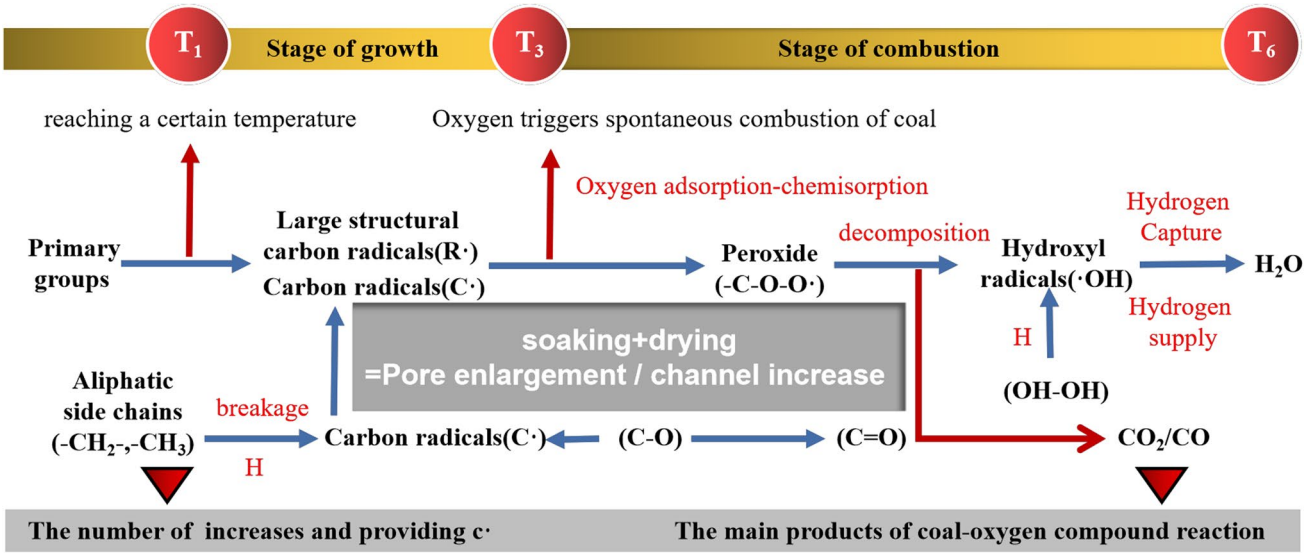

Fig. 11 Coal-oxygen composite mechanism model of water immersion drying

The primary mechanism is as follows: free radicals in coal absorb hydrogen atoms from the aliphatic hydrocarbons already present and produce C radicals. Due to the formation of adsorption sites for O_2, chemisorption occurs, releasing heat in the form of C radicals and producing peroxides (O–O–C) (Cheng et al. 2022). The free hydroxyl radicals and carbonyl groups are then produced due to a series of events in which the oxygen atoms in the peroxide connect with hydrogen atoms from neighboring aliphatic hydrocarbons to produce carbon dioxide, carbon monoxide gas, and carbon radicals. Moreover, hydroxyl groups absorb free hydrogen atoms of aliphatic hydrocarbons and oxygen-containing functional groups to create ·C radicals, CO, and H_2O. These reactions create ·C radicals and free hydroxyl groups in coal, which undergo continuous chemical adsorption reactions. Recent studies have shown that water immersion provides -OH and hydrogen ions to speed up peroxide formation and leads to constant pore crack development and changes in pore type. Drying further opens the pore channels and increases the contact area between coal and oxygen, thus promoting the coal-oxygen chain reaction.

4 Conclusions

(1) This study aimed to investigate coal's pore characteristics, chemical structure parameters, and activation energy during the spontaneous combustion heating process at different drying times following 30 days of immersion. The study also revealed the pore size variation characteristics and heating properties of dry coal samples immersed in water. The findings provide a theoretical foundation for developing prevention and control techniques for residual coal spontaneous combustion after water invasion in goaf.

(2) A comparative analysis of the thermal weight loss characteristics and activation energy of three characteristic stages during the spontaneous combustion heating process of five different coal samples showed that 36-S-Coal had a higher spontaneous combustion tendency than the other coal samples. This is because 36-S-Coal exhibited a higher T_2–T_6 characteristic temperature and a lower ignition activation energy than the other coal samples.

(3) The R-Coal pore type mainly comprises one-end closed impermeable pores. The surface is relatively flat and smooth, the number of pore cracks is small, the proportion of pore group area is low, and a small amount of gravel is attached to the coal surface and around the cracks. The pore type of 36-S-Coal is open pore. A large amount of gravel and minerals in the coal body are precipitated from the pores with the airflow, resulting in a large amount of gravel around the pore group, and the area of the pore group increases, and the porosity increases.

(4) Using infrared spectroscopy to analyze the two coal samples, it was found that soaking and drying did not change the functional group types of coal samples. However, the content of C = O, $-CH_3$, and intramolecular hydrogen bonds increased after soaking for 30 days and drying for 36 h. Further calculation of the degree of fat chain and chain length showed that the degree of the fat chain of 36-S-Coal was 1.56, and the degree of the fat chain of R-Coal was 1.86. This indicates that

the aliphatic chain structure of coal is changed after 36 h of drying after 30 days of soaking, resulting in the continuous shedding of residual coal aliphatic chain branches. The length of the aliphatic chain becomes shorter, which makes the skeleton of coal looser and the low-temperature oxidation reaction of 36-S-Coal easier.

(5) Based on the above experimental results, the formation of ·C free radicals, the generation of chemical adsorption sites of O_2, and the process of a further generation of peroxides were analyzed. The coal-oxygen composite mechanism of coal after water immersion drying was obtained, and it was shown that providing oxygen atoms and accelerating peroxide generation was the key to the whole process. The prevention and control technology and measures for the spontaneous combustion of water-immersed air-dried coal should strengthen the plugging of coal pores and prevent the generation of chemical adsorption points, thereby reducing the generation of peroxides.

Acknowledgements This work was supported by the financial support of the General Projects of National Natural Science Foundation of China (52074156).

Author contributions YL: Formal analysis, writing-original draft, visualization. hiyan wang: methodology, conceptualization, writing-review and editing. HN: Writing-original draft, visualization. TW: Methodology, conceptualization, writing-review & editing. ZC, YC: Investigation. QQ: Investigation. All authors read and approved the final manuscript.

Availability of data and materials Data will be made available on request.

Declarations

Competing Interests The authors declare that they have no known competing financial interests or personal relationships that could have appeared to influence the work reported in this paper.

References

Chen Y, Mastalerz M, Schimmelmann A (2012) Characterization of chemical functional groups in macerals across different coal ranks via micro-FTIR spectroscopy. Int J Coal Geol 104:22–33

Cheng G, Tan B, Zhang Z, Fu S, Haiyan W, Wang F (2022) Characteristics of coal-oxygen chemisorption at the low-temperature oxidation stage: DFT and experimental study. Fuel 315:123120

Choi H, Thiruppathiraja C, Kim S, Rhim Y, Lim J, Lee S (2011) Moisture readsorption and low temperature oxidation characteristics of upgraded low rank coal. Fuel Process Technol 92(10):2005–2010

Deng J, Zhao J, Zhang Y, Huang A, Liu X, Zhai X, Wang C (2016) Thermal analysis of spontaneous combustion behavior of partially oxidized coal. Process Saf Environ Protect 104:218–224

Deng J, Yang Y, Zhang Y-N, Liu B, Shu C-M (2018) Inhibiting effects of three commercial inhibitors in spontaneous coal combustion. Energy 160:1174–1185

Dey S (2012) Enhancement in hydrophobicity of low rank coal by surfactants—a critical overview. Fuel Process Technol 94(1):151–158

Fan Y-J, Zhao Y-Y, Hu X-M, Wu M-Y, Xue D (2020) A novel fire prevention and control plastogel to inhibit spontaneous combustion of coal: Its characteristics and engineering applications. Fuel 263:116693

Fang X, Wang H, Tan B, Wang F, Zhuang Shao Z, Cheng G, Yao H (2022) Experimental comparison study of CO_2 and N_2 inerted loose coal based on atmospheric pressure gas replacement. Fuel 328:125347

Fei Y, Abd Aziz A, Nasir S, Jackson WR, Marshall M, Hulston J, Chaffee AL (2009) The spontaneous combustion behavior of some low rank coals and a range of dried products. Fuel 88(9):1650–1655

Ghosh AK, Bandopadhyay AK (2020) Formation of thermogenic gases with coalification: FTIR and DFT examination of vitrinite rich coals. Int J Coal Geol 219:103379

He X, Liu X, Nie B, Song D (2017) FTIR and Raman spectroscopy characterization of functional groups in various rank coals. Fuel 206:555–563

Huang Q, Liu S, Wang G, Wu B, Yang Y, Liu Y (2019) Gas sorption and diffusion damages by guar-based fracturing fluid for CBM reservoirs. Fuel 251:30–44

Huang Z, Zhao X, Gao Y, Shao Z, Zhang Y, Liu X (2022) The influence of water immersion on the physical and chemical structure of coal. Combust Sci Technol 194(6):1136–1154

Jiang J, Zhang S, Longhurst P, Yang W, Zheng S (2021) Molecular structure characterization of bituminous coal in Northern China via XRD, Raman and FTIR spectroscopy. Spectrochim Acta Part A: Mol Biomol Spectrosc 255:119724

Li L, Fan H, Hu H (2017) Distribution of hydroxyl group in coal structure: a theoretical investigation. Fuel 189:195–202

Li J, Li Z, Yang Y, Niu J, Meng Q (2019) Insight into the chemical reaction process of coal self-heating after N2 drying. Fuel 255:115780

Li Z, Ren T, Li X, Qiao M, Yang X, Tan L, Nie B (2023) Multiscale pore fractal characteristics of differently ranked coal and its impact on gas adsorption. Int J Mining Sci Technol. https://doi.org/10.1016/j.ijmst.2022.12.006

Liang Y, Yang Y, Guo S, Tian F, Wang S (2023) Combustion mechanism and control approaches of underground coal fires: a review. Int J Coal Sci Technol 10(1):24. https://doi.org/10.1007/s40789-023-00581-w

Liu J, Yang X, Jiang X, Jiang X (2022) Pyrolysis mechanisms of coal extracts based on TG-FTIR and ReaxFF MD study. Fuel Process Technol 227:107124

Niu H, Liu Y, Wu K, Wu J, Li S, Wang H (2022) Study on pore structure change characteristics of water-immersed and air-dried coal based on SEM-BET. Combust Sci Technol. https://doi.org/10.1080/00102202.2022.2054272

Odeh AO (2015) Oualitative and quantitative ATR-FTIR analysis and its application to coal char of different ranks. J Fuel Chem Technol 43(2):129–137

Onifade M, Genc B (2018) Comparative analysis of coal and coal-shale intrinsic factors affecting spontaneous combustion. Int J Coal Sci Technol 5(3):282–294. https://doi.org/10.1007/s40789-018-0222-5

Pan J, Wang K, Hou Q, Niu Q, Wang H, Ji Z (2016) Micro-pores and fractures of coals analysed by field emission scanning electron microscopy and fractal theory. Fuel 164:277–285

Qi X, Li Q, Zhang H, Xin H (2017) Thermodynamic characteristics of coal reaction under low oxygen concentration conditions. J Energy Inst 90(4):544–555

Reich M, Snook I, Wagenfeld H (1992) A fractal interpretation of the effect of drying on the pore structure of Victorian brown coal. Fuel 71(6):669–672

Sensogut C, Ozdeniz A, Gundogdu I (2007) Temperature profiles of coal stockpiles. Energy Sources Part A: Recov Util Environ Effects 30(4):339–348

Shi Q, Qin B, Bi Q, Qu B (2018) An experimental study on the effect of igneous intrusions on chemical structure and combustion characteristics of coal in Daxing Mine, China. Fuel 226:307–315

Song F, Wang X, Li T, Zhang J, Bai Y, Xing B, Giesy JP, Wu F (2019) Spectroscopic analyses combined with Gaussian and Coats-Redfern models to investigate the characteristics and pyrolysis kinetics of sugarcane residue-derived biochars. J Clean Prod 237:117855

Tan B, Song X, Zhang B, Shao Z, Li Z, Liu S (2022) Study on the effect of different seawater mass ratio on coal spontaneous combustion characteristics. Thermochim Acta 716:179328

Thommes M, Kaneko K, Neimark AV, Olivier JP, Rodriguez-Reinoso F, Rouquerol J, Sing KS (2015) Physisorption of gases, with special reference to the evaluation of surface area and pore size distribution (IUPAC Technical Report). Pure Appl Chem 87(9–10):1051–1069

Wang D (2012) The coal oxidation dynamics: theory and application. Science Press, Beijing, pp 42–60

Wang H, Fang X, Du F, Tan B, Zhang L, Li Y, Xu C (2021) Three-dimensional distribution and oxidation degree analysis of coal gangue dump fire area: a case study. Sci Total Environ 772:145606

Wang G, Shi G, Yang Y, Liu S (2022) Experimental study on the exogenous fire evolution and flue gas migration during the fire zone sealing period of the coal mining face. Fuel 320:123879

Xiaowei Z, Bo W, Kai W, Obracaj D (2019) Study on the influence of water immersion on the characteristic parameters of spontaneous combustion oxidation of low-rank bituminous coal. Combust Sci Technol 191(7):1101–1122

Xu Y-L, Bu Y-C, Wang L-Y (2021) Re-ignition characteristics of the long-flame coal affected by high-temperature oxidization & water immersion. J Clean Prod 315:128064

Yang Y, Li Z, Si L, Gu F, Zhou Y, Qi Q, Sun X (2017) Study governing the impact of long-term water immersion on coal spontaneous ignition. Arab J Sci Eng 42:1359–1369

Yang F, Zhou A, Zhao W, Yang Z, Li H (2019) Thermochemical behaviors, kinetics and gas emission analyses during co-pyrolysis of walnut shell and coal. Thermochim Acta 673:26–33

Yu J, Tahmasebi A, Han Y, Yin F, Li X (2013) A review on water in low rank coals: the existence, interaction with coal structure and effects on coal utilization. Fuel Process Technol 106:9–20

Zeng Q, Shen L (2022) Experimental study on the oxidation kinetics of coal in typical coal mining areas of the Southern Junggar coalfield, Xinjiang, China. Int J Coal Sci Technol 9(1):78. https://doi.org/10.1007/s40789-022-00542-9

Zhang Y, Lebedev M, Sarmadivaleh M, Barifcani A, Rahman T, Iglauer S (2016) Swelling effect on coal micro structure and associated permeability reduction. Fuel 182:568–576

Zhang Q, Hu X-M, Wu M-Y, Zhao Y-Y, Yu C (2018) Effects of different catalysts on the structure and properties of polyurethane/water glass grouting materials. J Appl Polym Sci 135(27):46460

Zhang Y, Chen L, Zhao J, Deng J, Yang H (2019) Evaluation of the spontaneous combustion characteristics of coal of different metamorphic degrees based on a temperature-programmed oil bath experimental system. J Loss Prev Process Ind 60:17–27

Zhao J, Deng J, Wang T, Song J, Zhang Y, Shu C-M, Zeng Q (2019) Assessing the effectiveness of a high-temperature-programmed experimental system for simulating the spontaneous combustion properties of bituminous coal through thermokinetic analysis of four oxidation stages. Energy 169:587–596

Zhao J, Ming H, Guo T, Zhang Y, Deng J, Song J, Zeng Q, Shu CM (2022) Semi-enclosed experimental system for coal spontaneous combustion for determining regional distribution of high-temperature zone of coal fire. Int J Coal Sci Technol 9(1):62. https://doi.org/10.1007/s40789-022-00535-8

Zhong X, Kan L, Xin H, Qin B, Dou G (2019) Thermal effects and active group differentiation of low-rank coal during low-temperature oxidation under vacuum drying after water immersion. Fuel 236:1204–1212

Zhou F, Liu S, Pang Y, Li J, Xin H (2015) Effects of coal functional groups on adsorption microheat of coal bed methane. Energy Fuels 29(3):1550–1557